

## Unusual paramagnet to ferromagnet phase transition and magnetic inhomogeneities in hole doped manganites

*A.V.Lazuta, V.A.Ryzhov, I.A.Kiselev, Yu.P.Chernenkov, O.P.Smirnov, P.L.Molkanov, I.O.Troyanchuk\*, V.A.Khomchenko\**

St.Petersburg Institute for Nuclear Physics, Russian Academy of Sciences, Gatchina, 188300 St.Petersburg, Russia

\*Institute of Solid State and Semiconductor Physics, National Academy of Sciences of Belarus, 17 P.Brovki St., 220072 Minsk, Belarus

*Received November 12, 2007*

Results of structural neutron diffraction study, nonlinear magnetic response and magnetic resonance measurements are presented for insulating  $\text{La}_{0.88}\text{MnO}_{2.91}$  with  $T_C \approx 216$  K. The diffraction data are considered using the monoclinic  $P2/a$  and orthorhombic  $Pbnm$  space groups in a temperature range 4–300 K. The compound has been found to have the monoclinic structure at 300 K and orthorhombic one at 4 K. In the intermediate temperature range, these two phases coexist. According to the data on nonlinear response and magnetic resonance, this compound exhibits an unconventional paramagnetic (P) to ferromagnetic (F) phase transition. Below  $T^* \approx 247$  K, the usual P phase is transformed into a mixed state which is characterized by the appearance of the F regions in the P matrix. The temperature evolution of this state is very close to that found in the traditionally doped  $\text{Nd}_{1-x}\text{Ba}_x\text{MnO}_3$  ( $x = 0.23, 0.25$ ) manganites. This supports the supposition on universal character of this phenomenon, namely, formation of an inhomogeneous magnetic state above  $T_C$  with the coexistence of the P and F regions. The F domains are expected to exhibit a metallic state while the P phase is an insulator.

Результаты структурных нейтрон-дифракционных исследований, измерений нелинейного отклика и магнитного резонанса представлены для изолятора  $\text{La}_{0.88}\text{MnO}_{2.91}$  с  $T_C \approx 216$  К. Анализ дифракционных данных выполнен с использованием моноклинной и орторомбической пространственных групп в температурной области 4–300 К. Обнаружено, что соединение имеет моноклинную структуру при 300 К и орторомбическую при 4 К. Согласно данным нелинейного отклика и магнитного резонанса, манганит испытывает нетрадиционный парамагнетик (П) — ферромагнетик (Ф) фазовый переход. Ниже  $T^* \approx 247$  К обычная П фаза трансформируется в смешанное состояние, которое характеризуется появлением Ф областей в П матрице. Температурная эволюция этого состояния близка к эволюции, обнаруженной в манганитах  $\text{Nd}_{1-x}\text{Ba}_x\text{MnO}_3$  ( $x = 0,23, 0,25$ ) с традиционным допированием. Данное соответствие поддерживает предположение об универсальном характере формирования неоднородного магнитного состояния выше  $T_C$  с сосуществованием П и Ф областей. Ожидается, что Ф домены находятся в металлическом состоянии, тогда как П фаза является изолятором.

The interest in the study of the perovskite manganite oxides is due to their unusual physical properties. The hole-doped manganites can exhibit the colossal magnetoresistance effect (CMR) that is among the

central problems in the physics of these materials. They are traditionally doped by substituting a trivalent lanthanide for a divalent alkaline-earth ion. The doping usually causes a transition from an insulating (I)

antiferromagnetic to I ferromagnetic (F) state and then to F metallic phase. An important aspect of that behavior is the nature of a paramagnetic (P) to F phase transition and formation of an inhomogeneous magnetic state above  $T_C$ . This problem is still a matter of discussion [1, 2]. Recently, the study of nonlinear response to a weak *ac* magnetic field for  $\text{Nd}_{1-x}\text{Ba}_x\text{MnO}_3$  ( $x = 0.23, 0.25$ ) single crystals with a pseudocubic structure and the FI ground state has revealed an unusual scenario of the P-FI phase transition [3, 4]. Above  $T^*$  ( $\approx T_C + 20$  K), the material critical behavior corresponded to that of a 3D isotropic ferromagnetic. Below  $T^*$ , an anomalous behavior was observed characterized by the appearance of a new phase with the strong nonlinear properties in the weak magnetic fields. The resistivity of these compounds show a resistivity anomaly (plateau) near  $T_C$ . This suggests the quasi-metallic transport properties of the anomalous phase. A question arises whether this scenario of the P-F transition is universal for other manganites. To elucidate this problem, it is reasonable to study this transition in the compounds with another doping species.

A new class of the manganites  $\text{La}_{0.88}\text{MnO}_x$  ( $x = 2.82-2.95$ ), where the doping is caused by variation in the oxygen content, has been recently synthesized. The phase diagram, magnetic and transport properties of those compounds have been found to be similar to those of the traditionally doped manganites [5]. The preliminary study of  $\text{La}_{0.88}\text{MnO}_{2.91}$  manganite with the FI ground state revealed the scenario of P-F phase transition similar to that of the NdBa system [6]. At the same time, an essential difference in the anomalous phase properties, arising below  $T^* \approx 247$  K ( $> T_C \approx 216$  K), was found, namely, its nonlinear response has shown a strong field hysteresis.

We present here the results of careful investigations of the P-F phase transition in the  $\text{La}_{0.88}\text{MnO}_{2.91}$  compound. They include the detailed data on the second harmonic of magnetization  $M_2$  that makes it possible to study the nonlinear properties in weak fields. The magnetic resonance is used to examine the critical behavior of the compound at a higher constant field  $H$  and frequency ( $f \approx 8.37$  GHz) than in the experiments with  $M_2$ . At last, the neutron diffraction studies are performed to control the structural changes.

The best fit of neutron diffraction data indicates a competition between two structure. A monoclinic phase ( $P2/a$  space group) dominates from 290 K down to 200 K. Below 160 K, an orthorhombic ( $Pbnm$  space group) is the major phase. The differences between the structures in the dominating states are insignificant (see a discussion below). Thus, the compound exhibits only a weak structural reorganization. In addition, above  $T_C$ , the monoclinic phase completely dominates that excludes a question on a simple structural origination of the inhomogeneous magnetic state. The  $M_2$  data reveal a close similarity between temperature evolution of the  $H$ -hysteretic anomalous (A) phase of this compound and temperature behavior of the A phase of the NdBa system. The magnetic resonance measurements confirm the existence of the F regions below  $T^*$ . According to these and  $M_2$  data, the critical behavior of the major P phase corresponds to a ferromagnet exhibiting a second order phase transition.

The polycrystalline  $\text{La}_{0.88}\text{MnO}_x$  sample was prepared by solid-state reaction using high purity  $\text{La}_2\text{O}_3$  and  $\text{Mn}_2\text{O}_3$  reagents. To remove absorbed water, the  $\text{La}_2\text{O}_3$  was precalcined ( $1000^\circ\text{C}$ , 1 h). Then the compacted mixture of reagents taken in stoichiometric cation ratio was heat annealed at  $950^\circ\text{C}$  for 2 h. The obtained product was ground, pressed into pellets, annealed at  $T = 1300^\circ\text{C}$  in air for 6 h and then cooled at a rate of  $30^\circ\text{C}/\text{h}$  down to room temperature. The oxygen content of the resulting material has been determined using thermogravimetric analysis, i.e. the decomposition of the sample into simple oxides  $\text{La}_2\text{O}_3$  and  $\text{MnO}$  in a reducing  $\text{H}_2/\text{N}_2$  flow. The true chemical formula of the obtained compound was  $\text{La}_{0.88}\text{MnO}_{2.96}$  with an estimated error of  $\pm 0.01$  oxygen per formula. To prepare the  $\text{La}_{0.88}\text{MnO}_{2.91}$  compound, the oxygen was reduced by calcination in evacuated quartz ampoules at  $T = 1050^\circ\text{C}$  for 24 h with metallic tantalum as the reducing agent. All the samples were quenched. The oxygen loss has been checked by the weighing of the samples before and after the reduction.

The diffraction experiments were performed on the 48-counter PNPI powder neutron diffractometer (Ge monochromator,  $\lambda = 1.383$  Å) in a cryostat at 4.2–300 K. The neutron diffraction data were processed using the FullProf program [7] that is a recent development of the FULLPROF software. The second harmonics of the longitudinal magnetization  $M_2$  in a nonlinear re-

sponse were measured in parallel *dc*- and *ac*-harmonic magnetic fields  $H(t) = H + h\sin\omega t$  ( $h \leq 35$  Oe,  $f = \omega/2\pi = 15.7$  MHz). The  $\text{Re}M_2(H)$  and  $\text{Im}M_2(H)$  parts of the  $M_2$  were simultaneously recorded as the functions of a constant magnetic field  $H$  for various sample temperatures ( $T = 85$ – $315$  K). This field was scanned symmetrically relative to the point  $H = 0$  to detect the field hysteresis of the signal. The  $H$  scan amplitude was 300 Oe. We used the sample shaped as a thin plate ( $V \approx 2 \times 1.2 \times 0.11(2)$  mm<sup>3</sup>,  $m \approx 1.6$  mg), the magnetic field being oriented parallel to its plane. This allowed us to avoid the temperature gradient inside the sample. The setup and method of separation of the  $M_2$ -phase components have been described elsewhere [8]. The sensitivity of these measurements was about  $10^{-9}$  emu.

In ESR study, we used also the thin plate sample ( $V \approx 2 \times 2 \times 0.2$  mm<sup>3</sup>,  $m \approx 4$  mg) for the same reason as in the  $M_2$  measurements. We employed a home-built X-range ESR spectrometer ( $f = 8.37$  GHz) described earlier, using a cylindrical balance cavity with the TE<sub>111</sub> type of oscillations [9]. It registers the component of the sample magnetization which is proportional to the off-diagonal part of its magnetic dynamic susceptibility [ $M_y(\omega) = \chi_{yx}(\omega)h_x(\omega)$ ], with a linear-polarized exciting *ac*-field  $\mathbf{h} \parallel \text{Ox}$  and constant field  $\mathbf{H} \parallel \text{Oz}$  (Oz is a cylindrical axis of the cavity) and allows one to avoid the problems associated with absorption in zero field due to relaxation in a critical paramagnetic regime. The sample was placed on the cavity bottom and  $\mathbf{H}$  was directed perpendicular to the sample plane.

Below  $T^* \approx 247$  K, the nonlinear response of the compound reveals features of a phase separated (PS) magnetic state with  $F$  moment in the anomalous phase that signals the first order transition [6]. It is natural, therefore, to expect a temperature hysteresis of the ESR signal. Besides, the state being formed at the PS usually depends on the process used to transfer a system in the PS regime. Therefore, several types of the temperature scan with/without an external magnetic field were performed: (I) the sample was slowly cooled at  $H = 0$  from room temperature down to 160 K below  $T_C$  (ZFC regime) and then slowly heated (ZFH regime) back to room temperature. In the chosen temperature points ( $T$  points), the ESR spectra were recorded. A temporal stabilization time before recording the signal was about 200 to 300 s at each  $T$  point; (II) the

same temperature scan as above was applied but in  $H = 4$  kOe during cooling or heating between  $T$  points (FC and FH regimes, respectively). This procedure also tests a possible PS state and properties of phases because the magnetic field can change a balance between the phase fractions; (III) A fast cooling of the sample was used down to 160 K in zero  $H$  and then the sample was slowly heated up to room temperature (FZFC regime).

The measured diffraction profiles for 4–300 K are found to be well fitted using a two-phase structural model. It includes the monoclinic  $P2/a$  and orthorhombic  $Pbnm$  phases. The monoclinic structure dominating at room temperature is transformed into the orthorhombic phase with lowering temperature. Figs. 1, 2 show the temperature dependences of the structural parameters, the relative volume fractions, and the magnetizations for these phases. The monoclinic-orthorhombic transition is seen to develop below  $T_{MO} \sim 230$  K and to be completed at 100 K (Fig. 1a). This agrees with results of [5] where  $T_{MO}$  was found to decrease with increasing  $x$  from 650 K ( $x = 2.81$ ) down to 450 K ( $x = 2.84$ ). The monoclinic structure is characterized by two Mn sites, which produce a layer arrangement of two different MnO<sub>6</sub> octahedra along the  $a$  axis. As the data on the Mn–O bond lengths show (Fig. 2c), the octahedra exhibit the Jahn-Teller (JT) distortions which are small at room temperature and increase at cooling. There is a difference in the splitting of the bond lengths. In Mn1-site, the long bond (Mn1–O21) lies in the  $bc$  plane and it increases with decreasing temperature. In Mn2 site, the  $bc$  plane is occupied by the short bond (Mn2–O21) which decreases on cooling. Two other bond lengths approximately coincide in both sites and depend weakly on temperature.

A small amount of the orthorhombic phase is observed from 300 K down to  $T_{M-O} \sim 230$  K where its fraction is about 12 %. In this temperature range, the phase structural parameters exhibit the temperature-dependent variations (Fig. 1b, Figs. 2a, 2b) that correspond to the initial stage of its formation. Below  $T_{MO}$ , the structural parameters become stable. The Mn–O bond lengths are almost equal in this range.

The  $F$  order is developed in both phases at close temperatures:  $T_{CM} \approx 220$  K and  $T_{CO} \approx 200$  K for the monoclinic and orthorhombic structures, respectively (Figs. 2b, 2d). The  $T_{CM}$  for the major phase agrees

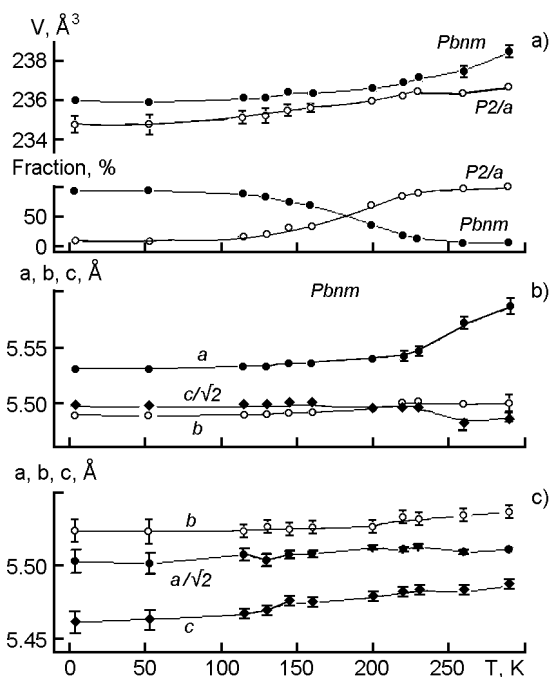


Fig. 1. Temperature dependences of the unit cell parameters  $a$ ,  $b$ ,  $c$  [panels (b), (c)], the unit cell volume,  $V$ , and the volume fraction [panel (a)] for the structural phases  $Pbnm$  and  $P2/a$ .

reasonably with  $T_C \approx 216$  K obtained from the data on a third harmonic of magnetization obtained at low frequency (20 kHz) of the exciting  $ac$  field [6]. The temperature dependence of the F moment for the orthorhombic phase shows a behavior typical for a ferromagnet. The magnetic moment at 4 K ( $3.4\mu_B$ ) is close to that ( $3.7\mu_B$ ) expected for mixture of the  $Mn^{3+}$  and  $Mn^{4+}$  ions corresponding to  $x = 2.91$ . The magnetization of the monoclinic phase increases monotonously at cooling from  $T_{CM}$  down 130 K. At 115 K, it reduces slightly and remains at the same level down to 4 K. This occurs when a fraction of this phase becomes small (12 % at 130 K). Therefore, this behavior may be related to formation of small fragments of the phase which cannot support the well-ordered state as the bulk material.

Note the following important features in the  $T$ -evolution of the structure. The monoclinic phase dominates above 200 K. The JT distortions, which account for the difference between two Mn sites, are small in this region i.e., these sites are almost equivalent. Moreover, the Mn–O bond lengths in this phase are close to those in the orthorhombic structure in its weakly temperature-dependent state (below 230 K). The same closeness exists between the Mn–O–Mn an-

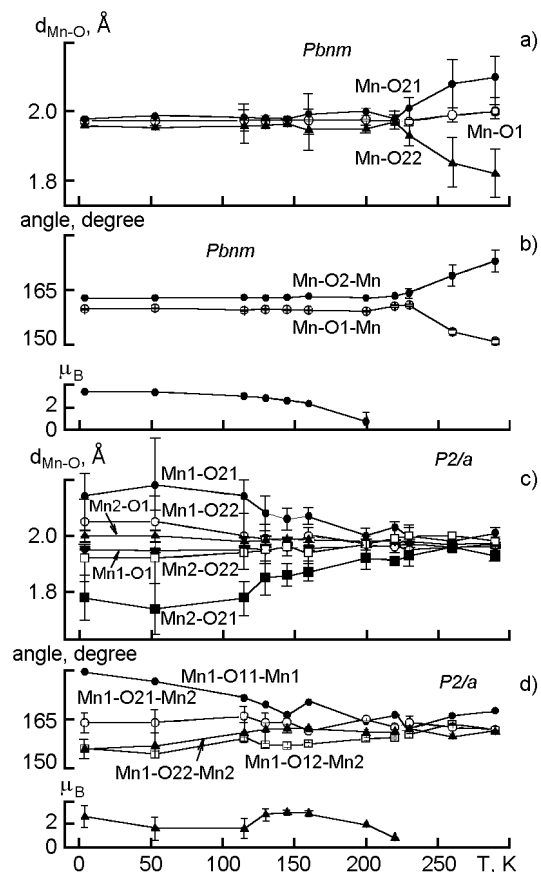


Fig. 2. Temperature dependences of the Mn–O bond lengths [panels (a), (c)]; Mn–O–Mn angles and magnetic moments per Mn ion [panels (b), (d)] for the  $Pbnm$  and  $P2/a$  structural phases, respectively.

gles. As a result, the compound as a whole is transformed weakly with temperature, remaining near to an orbital disordered state. This explains why the structural changes can have little effect on the magnetic properties.

To clarify the critical behavior above  $T_C$ , the second harmonic of magnetization,  $M_2(T)$ , was investigated under condition  $M_2 \propto h^2$  when the longitudinal response is described by the second order dynamic susceptibility  $\chi_{||}^{(2)}(\omega, H, T)$ . The properties of this function were considered in [3]. Fig. 3 displays the  $\text{Re}M_2(H)$  and  $\text{Im}M_2(H)$  dependences for some characteristic temperatures that are related to the three ("impurity", normal and anomalous)  $T$  ranges with different  $M_2(H, T)$  dependences. Similar ranges were found for the NdBa system [3, 4]. In the "impurity" range (315–285 K), an essentially  $T$ -independent signal is observed. It exhibits a weak  $H$ -hysteresis with a small  $M_2$  at  $H = 0$  that provides a clear evidence

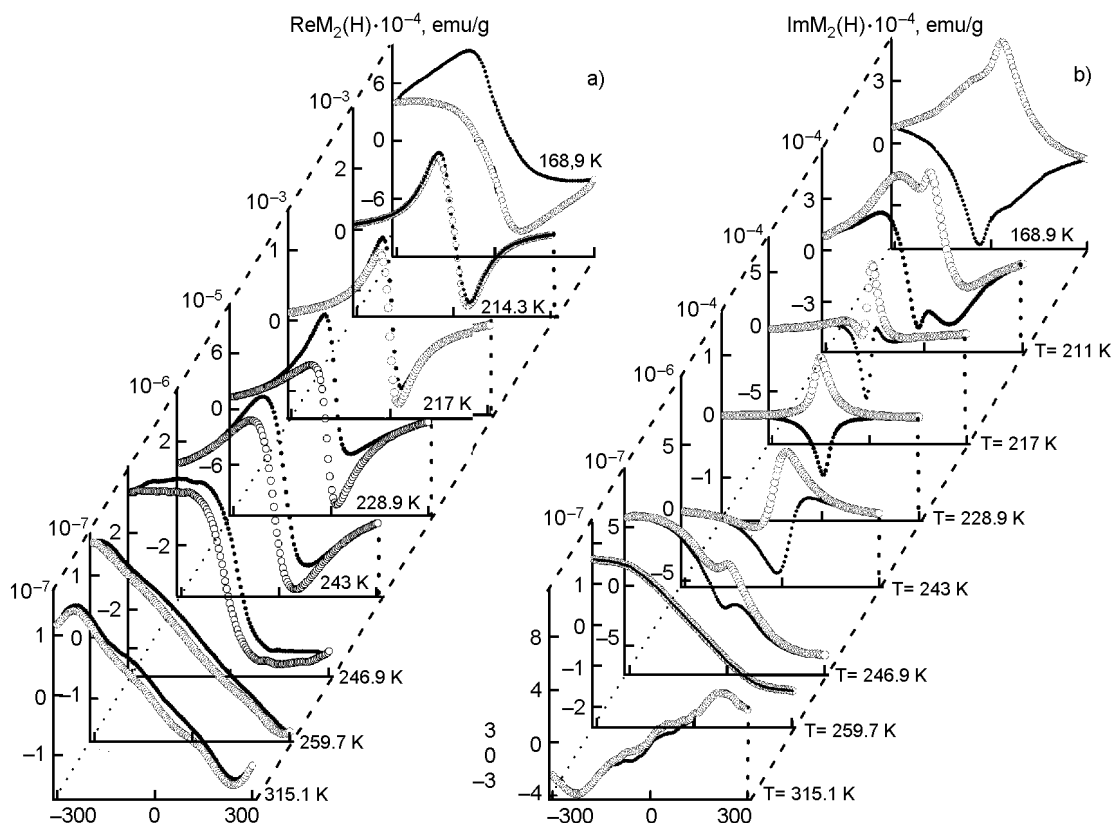


Fig. 3. Two phase components of the second harmonic of magnetization  $M_2$  as functions of the constant magnetic field  $H$  at some temperatures. Full (smaller size) and open symbols are used for curves recorded at the direct and reverse  $H$ -scans, respectively.

of a spontaneous magnetization in this phase. Indeed,  $M_2$  is a pseudo-vector and even function of  $h$ . Therefore,  $M_2(H)$  is odd in  $H$  with  $M_2(0) = 0$  in the paramagnetic phase. Accordingly, the response with  $M_2(0) \neq 0$  in the "impurity" range is associated with a small amount of a magnetically ordered impurity phase.

In the normal range ( $285\text{--}247\text{ K} \approx T^*$ ), the signal starts to increase with decreasing temperature, and we observe the typical response that can be attributed to a 3D isotropic ferromagnet in weak fields  $g\mu H \ll T_C \tau^{5/3}$  ( $\tau = (T - T_C)/T_C$ ). In this regime,  $\text{Re}M_2(H) \propto H$  and  $\text{Im}M_2(H)$  depend on  $H$  almost linearly [3, 4]. An example of this behavior is the data at  $259.7\text{ K}$  (see Fig. 3). The anomalous range ( $T^* = 247\text{ K} - T_C = 216\text{ K}$ ) is characterized by the appearance of an unexpected additional signal with extraordinary  $\text{Im}M_2(H)$  dependence (a hysteresis loop at  $H \leq 100\text{ Oe}$  with an extreme in a very weak field  $H \sim 10\text{ Oe}$ ), see Fig. 3b. The new signal increases sharply at cooling whereas the field position of its extreme remains weakly  $T$ -dependent down to

$T_C$  (Fig. 4b). This behavior can be attributed to an increase in volume of the new (anomalous) phase. In the  $\text{Re}M_2(H)$  dependence, the anomalous (A) signal also accounts for formation of the extreme at the small fields and field hysteresis (Fig. 3a). The field position of the minimum at  $H > 0$  ( $H_{min}$ ) decreases and extreme value of the  $\text{Re}M_2(H)$  ( $-\text{Re}M_{2min}$ ) increases with decreasing temperature (Figs. 4a, 4b). For this component,  $H_{min}$  changes with temperature since  $\text{Re}M_2$  is the sum of the comparable signals from the A and normal paramagnetic phases. The temperature dependences of the  $\text{Im}M_{2min}$ ,  $\text{Re}M_{2min}$  and  $H_{min}(\text{Re}M_2)$  show extremes approximately at  $T_C$  (Fig. 4). The value of  $H_{min}(\text{Im}M_2)$  begins to depend on temperature below  $T_C$  (Fig. 4b). It is remarkable that all the main peculiarities of the  $T$ -evolution of the  $H_{min}$  and  $M_{2min}$  for  $\text{Re}M_2$  and  $\text{Im}M_2$  coincide with those of  $\text{Nd}_{0.75}\text{Ba}_{0.25}\text{MnO}_3$  [4]. The new specific feature of this manganite is the hysteretic behavior of the A phase. It is characterized by the appearance of the signal at  $H = 0$  which is the consequence of

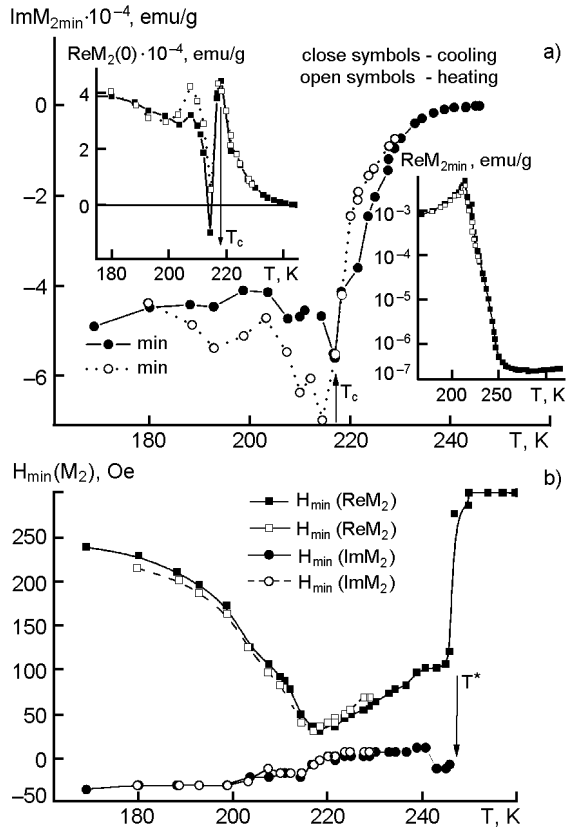


Fig. 4. Temperature dependences of  $\text{Re}M_2(H)$  and  $\text{Im}M_2(H)$  parameters in the cooling (closed symbols) and heating (open symbols) regimes. Panel (a) presents  $T$ -behavior of  $\text{Im}M_2(H)$  at its minimum. Insets 1 and 2 show the  $\text{Re}M_2(T)$  at  $H = 0$  and  $-\text{Re}M_2(H)$  at its minimum, respectively. Panel (b) displays  $T$ -evolution of the  $H$ -positions of the minima in  $\text{Re}M_2(H)$  and  $\text{Im}M_2(H)$ .

the spontaneous magnetization of this phase. Fig. 4a displays  $T$ -dependence of  $\text{Re}M_2(0, T)$  which, above  $T_C$ , arises due to the A phase. This signal increases with decreasing temperature down to  $T_C$ , reflecting the growing volume of this phase. A narrow hole extremum observed just below  $T_C$  is due to development of magnetization in the paramagnetic phase. In NdBa system,  $\text{Re}M_2(0, T)$  exhibits a strong negative peak at  $T_C$  [4]. In our case, this signal is combined with the positive contribution of the A phase.

Thus, the magnetically inhomogeneous state is formed below  $T^*$  which is characterized by the presence of ferromagnetic regions in paramagnetic matrix. A similar inhomogeneous state is found in the NdBa system above  $T_C$  where the A phase possesses the strong nonlinear behavior in the weak magnetic fields. In these compounds,

however, the strong  $H$ -hysteretic characteristics are not observed. The matter is that the F regions can behave as superparamagnetic particles when these regions are the single-domain clusters. There are no hysteretic effects in this regime. The superparamagnetic state is realized at temperatures above the so-called blocking temperature  $T_B$ . Below  $T_B$ , the magnetic behavior becomes hysteretic [8]. Since the  $T_B$  is proportional to activation energy  $K_A N_{at}$  ( $K_A$  is the effective magnetic anisotropy,  $N_{at}$  is the number of the atoms in the particle) it is material-dependent. As a result,  $T_B$  can be lower than 130 K in NdBa system and reaches 250 K in our case. The slow cooling and slow heating regimes were applied to check the temperature hysteresis of the  $M_2$  response. As Fig. 4a shows, the  $T$ -hysteresis is observed below  $T^*$  mainly in  $\text{Im}M_2(T, H)$  component where contribution of the A-phase is larger. This is in agreement with the first order character of its origination.

To examine the magnetic behavior of  $\text{La}_{0.88}\text{MnO}_{2.91}$  at a higher frequency (8.37 GHz) and higher magnetic fields ( $\sim 3$  kOe), the magnetic resonance has been studied in the temperature region 180–328 K. Fig. 5 displays the typical spectra for some temperatures obtained at the different  $T$ -scans. Similar spectra were also observed for other temperatures above  $T_C$ . Those are insensitive to different treatments for temperatures above approximately 241 K, reflecting the sample paramagnetic state. In this  $T$ -region, the spectra are well fitted by a Lorentzian line shape:

$$\chi_{as}(\omega, H) = \frac{1}{2}\chi \left\{ \left[ \frac{\omega\Gamma}{(\omega - g\mu H)^2 + \Gamma^2} - \frac{\omega\Gamma}{(\omega + g\mu H)^2 + \Gamma^2} \right] \cos\varphi_s - \left[ \frac{\omega(\omega - g\mu H)}{(\omega - g\mu H)^2 + \Gamma^2} - \frac{\omega(\omega + g\mu H)}{(\omega + g\mu H)^2 + \Gamma^2} \right] \sin\varphi_s \right\}, \quad (1)$$

as panel 1 of Fig. 5 shows. Here,  $\chi_{as}$  is the antisymmetric component of the sample dynamic susceptibility;  $\chi$  is the static susceptibility; and  $\varphi_s$  is the signal phase. Since the spin relaxation rate  $\Gamma$  is relatively large, the both circularly polarized components of  $ac$ -field are taken into account in Eq.(1). For this reason, a control sample (a polycrystalline stable nitroxyl radical with  $g = 2.055$  and  $\Gamma \approx 60$  Oe) was used to tune the phase of  $ac$ -field which is the reference point for  $\varphi_s$ . The fitting parameters in

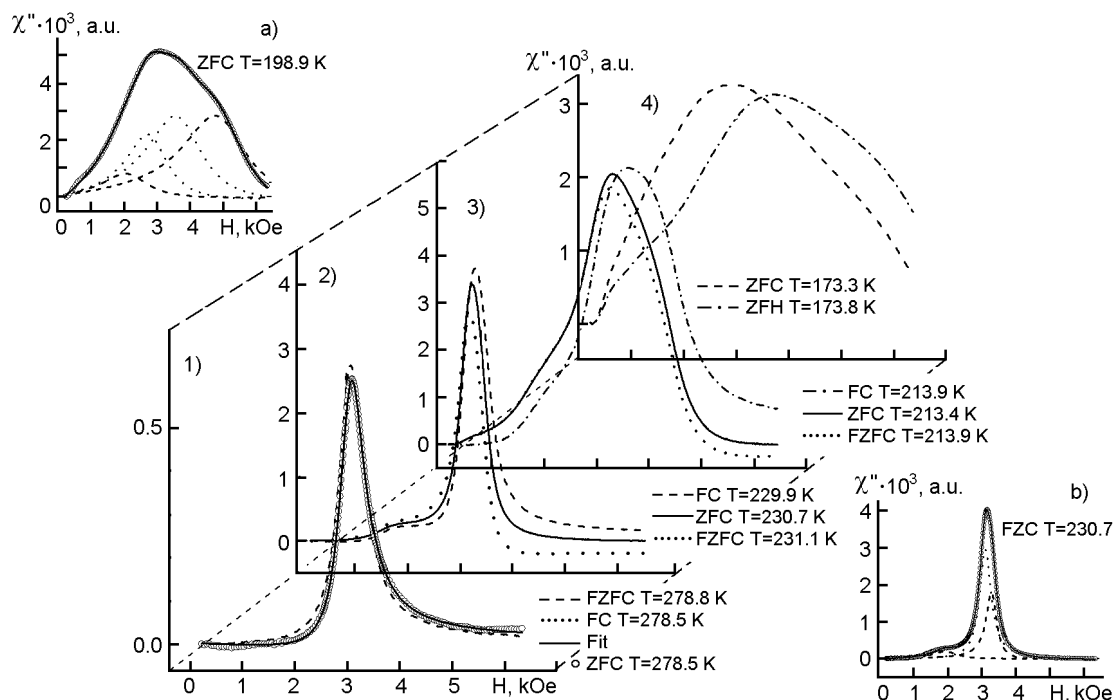


Fig. 5. Electron magnetic resonance spectra at some temperatures of the sample for different  $T$  treatments: (i) slow cooling at  $H = 0$  (ZFC, solid line or circles) and at  $H = 4$  kOe (FC, dash); (ii) slow heating after slow cooling at  $H = 0$  (ZFH, dash dot line) and after fast cooling at  $H = 0$  (FZFC, dot line); (iii) fit of the spectrum obtained at  $T = 278.5$  K in ZFC regime (solid line). Insets (a) and (b) present the fits of the spectra obtained below  $T_C$  and  $T^*$ , respectively.

Eq.(1) are  $\Gamma$ ,  $g$ ,  $\phi_s$  and the amplitude of the signal  $A_{as}(T) \propto \chi$ .

At a further decreasing  $T$ , below 241 K, the distinction between the spectra obtained at different  $T$ -scans increases. Besides, in the region  $241 \text{ K} > T > T_C$ , a "shoulder" at low field and a kink at high field arise (see inset (b) of Fig. 5). This is a ferromagnetic resonance from the A phase with the spontaneous magnetization which exhibits the characteristic splitting due to a magnetic anisotropy. To describe the signal in this region, we use three Lorentzians. The inset (b) of Fig. 5 presents this fit obtained at zero field cooling regime at 230.7 K. The dotted line displays the signal of the paramagnetic phase, the two dashed lines correspond to the A phase, and the circles present the recorded signal the solid line is the recorded summary spectrum. Below  $T_C$ , where the magnetic ordering is developed in the major paramagnetic phase, the fit becomes worse. To demonstrate sensitivity of the data to the ordering of the initial paramagnetic phase. Therefore, we need to add fourth Lorentzians in fitting function to improve fit. This result of the fit at

$T = 198.9$  K (the zero field cooling regime) is presented in the inset (a) of Fig. 5.

Fig. 6 displays the parameters of the MR-spectra  $H_{res}(T)$ ,  $\Gamma(T)$  and  $A_s(T)$  obtained in various  $T$ -regions. The regions correspond to the P state (1), P+F state (2), and F state (3). The paramagnetic phase signal at  $T \rightarrow T_C$  shows the usual behavior corresponding to a ferromagnetic exhibiting a second order phase transition. The  $A_s(T)$  ( $\propto \chi$ ) increases at  $T \rightarrow T_C$  and  $\Gamma(T)$  shows the critical enhancement (the inset of Fig. 6b). As the data on  $H_{res}(T)$  demonstrate, the ferromagnetic A phase appears above  $T_C$  and persists below  $T_C$ . Thus, even the F state remains inhomogeneous, at least above 200 K. A noticeable  $T$ -hysteresis is observed only below  $T_C$ . The region above  $T_C$  corresponds to the structure where the monoclinic phase dominates. Besides, the difference between the two manganite sites in this region is small and this structure is close to the orthorhombic one. This explains why the possible anomalies related to the structural two-phase state are not found.

Let us consider the possible reasons for formation of this inhomogeneous magnetic

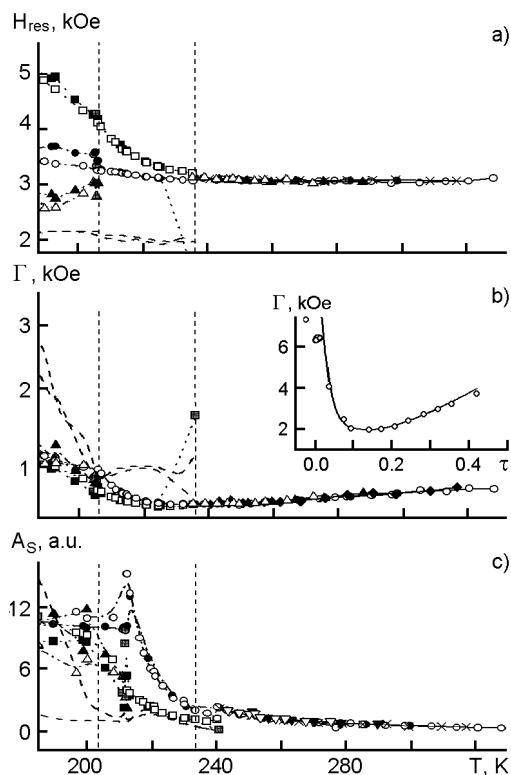


Fig. 6. Temperature dependences of the resonance field,  $H_{res}$  — panel (a); the relaxation rate of magnetization,  $\Gamma$  — panel (b); and amplitude of the signal,  $A_S$  — panel (c) for different temperature regimes (close symbols — slow cooling; open symbols — slow heating after slow cooling). In  $T$ -range 1 ( $330\text{ K} > T > 241$ ), the spectra parameters are found from fit by one Lorentzian for cooling at  $H = 0$  (ZFC — circles), for cooling at  $H = 4$  kOe (FC — triangles down), and for slow heating after fast cooling (FZFC — crosses). In  $T$ -ranges 2 ( $241\text{ K} \geq T > 211\text{ K}$ ) and 3 ( $211\text{ K} \geq T \geq 199\text{ K}$ ), the fits by three and four Lorentzians, respectively (see the text) are employed, and the parameters are displayed only for the ZFC and ZFH regimes and parameters are displayed. Stars and squares are used for two lines of the normal phase; circles and triangles up correspond to two lines of the anomalous phase.

state above  $T_C$ . Note first, that the state exists in the manganites with quite different doping characters. Second, it arises in different crystal structures with orthorhombic and monoclinic symmetries. This suggests a mechanism that is insensitive to these features. Recently, such a mechanism has been considered to explain the electronic inhomogeneities in the ground state of the F manganites [9]. It is known that the F ground state of the doped manganites is, generally speaking, inhomogeneous. The

F metallic state can contain insulating regions and the F insulating state can include metallic domains. These electronic inhomogeneities were studied using a model with Coulomb interactions between two electronic fluids — one localized (polaronic), the other extended (metallic) — and dopant ions. The long-range Coulomb interactions frustrate phase separation induced by the large on-site repulsion between the fluids. A phase arises which is inhomogeneous at a nanoscale. This mechanism explains why the otherwise phase separated state is broken into the state with nanoscale inhomogeneities, and can be relevant above  $T_C$ . However, the reason for the appearance of the mixed PI+FM state below  $T^*$  is still an open question.

To conclude, the presented results of thorough investigations of the P–F phase transition in the  $\text{La}_{0.88}\text{MnO}_{2.91}$  compound doped by oxygen nonstoichiometry with the FI ground state evidence the scenario which is qualitatively similar to that ion of the  $\text{Nd}_{1-x}\text{Ba}_x\text{MnO}_3$  ( $x = 0.23, 0.25$ ) crystals [3, 4]. Formation of the F regions in the paramagnetic matrix below  $T^* \approx 247\text{ K}$  is detected by nonlinear response to  $ac$ -field and the magnetic resonance. The mixed state originates by the first order fashion, the F clusters revealing the strong nonlinear properties in the weak fields. According to [5], a peculiarity (plateau) in the resistivity occurs in the  $\text{La}_{0.88}\text{MnO}_{2.91}$  near  $T_C$  that indicates the metallic character of the F domains. The obtained results suggest that appearance of the inhomogeneous magnetic state above  $T_C$  can be the universal phenomenon for the doped F manganites.

*Acknowledgments.* We are grateful to Dr. V.P.Khavronin for helpful discussions. This work was supported by the Russian Foundation for Basic Research, Grant No.06-02-17258-a.

## References

1. M.B.Salamon, M.Jaime, *Rev. Mod. Phys.*, **73**, 583 (2001).
2. E.Dagotto, T.Hotta, A.Moreo, *Phys. Rep.*, **344**, 1 (2001).
3. V.A.Ryzhov, A.V.Lazuta, I.D.Luzyanin et al., *Zh. Eksp. Teor. Fiz.*, **121**, 678 (2002).
4. V.A.Ryzhov, A.V.Lazuta, V.P.Khavronin et al., *Solid State Commun.*, **130**, 803 (2004).
5. I.O.Troyanchuk, V.A.Khomchenko, M.Tovar et al., *Phys. Rev. B*, **69**, 054432 (2004).
6. V.A.Ryzhov, A.V.Lazuta, I.A.Kiselev et al., *JMMM*, **300**, e159 (2006).
7. J.Rodríguez-Carvajal, *CPD Newsletter*, **26**, 12 (2001).



8. S.V.Vonsovskij, Magnetizm, Nauka, M. (1971) [in Russian].

9. V.B.Shenoy, T.Gupta, H.R.Krishnamurthy, T.V.Ramakrishnan, *Phys. Rev. Lett.*, **98**, 097201 (2007).

**Незвичайний фазовий перехід  
від парамагнітної до феромагнітної фази  
та магнітні неоднорідності у дірково-допованих  
манганітах**

***А.В.Лазута, В.А.Рижов, І.А.Кисельов, Ю.П.Черненко,  
О.П.Смирнов, П.Л.Молканов, І.О.Троянчук, В.А.Хомченко***

Представлено результати структурних нейтронно-дифракційних досліджень, вимірювань нелінійного відгуку та магнітного резонансу для ізолятора  $\text{La}_{0.88}\text{MnO}_{2.91}$  з  $T_C \approx 216$  К. Аналіз дифракційних даних виконано із застосуванням моноклінної та орторомбічної просторових груп у температурній області 4–300 К. Виявлено, що сполука має моноклінну структуру при 300 К та орторомбічну при 4 К. Згідно з даними про нелінійний відгук та магнітний резонанс, манганіт зазнає нетрадиційного фазового переходу парамагнетик (П) — феромагнетик (Ф). Нижче  $T^* \approx 247$  К звичайна П фаза трансформується у змішаний стан, який характеризується появою Ф областей у П матриці. Температурна еволюція цього стану є близькою до еволюції, виявленої у традиційно допованих манганітах  $\text{Nd}_{1-x}\text{Ba}_x\text{MnO}_3$  ( $x = 0,23, 0,25$ ). Ця відповідність підтверджує припущення про універсальний характер магнітного стану вище  $T_C$  зі співіснуванням П та Ф областей. Очікується, що Ф домени перебувають у металічному стані, в той час як П фаза є ізолятором.